

Table 1. ^1H NMR Spectra of Poly(PEG₈₀₀₀-lysine-stearylamine)

polymer	ratio of PEG protons to CH ₂ protons of stearyl groups	
	calcd	exptl
S28	22.6	28.0
S68	22.6	24.9
S113	22.6	25.3

ammonium salt (di-BOC lysine DCA) and *N*-hydroxysuccinimide were purchased from Sigma. Stearylamine, dicyclohexyl carbodiimide (DCC), dimethyl amino pyridine (DMAP), and triethylamine were purchased from Aldrich. All solvents were analytical grade. All materials were used as received, except for PEG 8000, which was azeotropically dried prior to use.

Methods. Synthesis of Lysine Stearylamine Dihydrochloride. A 25 g (47.3 mmol) sample of di-BOC lysine DCA was slurried with 150 mL of ethyl acetate and 100 mL of deionized water. Then, 150 mL of 1 M citric acid was added, and the mixture was agitated vigorously. Free acid was extracted from the aqueous phase four times with 50 mL of ethyl acetate. The organic phase was then washed four times with 50 mL of deionized water, dried over MgSO₄, evaporated under reduced pressure, and vacuum-dried to give 16.02 g (98%) of di-BOC lysine free acid as a bright white hygroscopic solid. A 16.0 g (46.2 mmol) sample of di-BOC lysine free acid, 12.4 g (46.0 mmol) of stearylamine, 0.366 g (3.24 mmol) of DMAP, and 9.5 g (45.9 mmol) of DCC were dissolved in 250 mL of methylene chloride and stirred for 20 h. The reaction mixture was filtered to remove *N,N*-dicyclohexyl urea (DCU), washed four times with 50 mL 0.5 M sodium bicarbonate, 50 mL 0.2 N HCl, and 50 mL saturated NaCl solution, and dried over MgSO₄. The solution was then concentrated under reduced pressure and subjected to flash silica gel chromatography to yield 20.9 g (76%) of di-BOC lysine stearylamine as bright white crystals. Then, 19.7 g (32.9 mmol) of di-BOC lysine stearylamine was dissolved in 100 mL of methylene chloride and 35 mL of 1 M HCl in anhydrous ethyl ether and stirred at room temperature for 24 h. The solution was evaporated to dryness and the resulting pale white solid (lysine stearylamine dihydrochloride) was dried under vacuum at room-temperature overnight. Materials were recrystallized in a 3:1 acetone/methanol mixture.

Synthesis of Bis(succinimidyl oxycarbonyl PEG) (BSC-PEG). The synthesis followed published procedures.^{13,14} The polydispersity of BSC-PEG 8000 (as determined by GPC relative to monodisperse PEG standards) was below 1.15.

Synthesis of Poly(PEG₈₀₀₀-lysine-stearylamine). Lysine stearylamine dihydrochloride was polymerized interfacially with BSC-PEG 8000 in the presence of potassium carbonate according to a published procedure.¹³

Characterization of Poly(PEG₈₀₀₀-lysine-stearylamine). ^1H NMR spectra in CDCl₃ were recorded on a Varian XL-200 spectrometer: δ 6.2 (1 H, br m, NH of stearyl group), 5.0 (1 H, m, ϵ -NH of lysine), 4.15–4.25 (4 H, terminal CH₂ of PEG), 3.6 (725 H, PEG overlapping with α -CHNH), 3.1 (4 H, m, ϵ -CH₂NH overlapping with CH₂NH of stearyl group), 1.31–1.8 (6 H, br m, CH₂ of lysine), 1.1–1.3 (32 H, all remaining CH₂ of stearyl group), 0.85 (3 H, t, CH₃ of stearyl group). Ratio of the integration of the PEG protons (δ 3.6) to the protons of the CH₂ of the stearyl group (δ 1.1–1.3) (Table 1) was found to be close to, although slightly higher than, the expected value for a 1:1 adduct of PEG 8000 to lysine stearylamine. For the sample referred as S28, in particular, the integration reveals a slight excess of PEG. This may indicate that there are more PEG groups than lysine-stearylamine groups terminating the chain and/or that there is a small amount of unreacted PEG 8000.

Molecular weights were determined by GPC using a Waters model 510 pump, two PL-gel GPC columns (pore size 10⁵ and 10⁴ Å), a Waters model 410 RI detector, and a Digital Venturis 466 computerized station using Millenium software. The mobile phase was DMF containing 0.1% (w/v) LiBr at a flow rate of 0.8 mL/min. The weight and number-average molecular

weights were determined relative to poly(ethylene oxide) standards.

$$\text{S28: } M_w = 28\,000; M_n = 18\,000$$

$$\text{S68: } M_w = 68\,000; M_n = 42\,000$$

$$\text{S113: } M_w = 113\,000; M_n = 74\,000$$

For S68 and S113, the chromatographs show a very small shoulder at the low molecular foot of the distribution, due to a small amount of unreacted PEG 8000. This contribution was not resolved from the main distribution for S28.

Characterization of Associative Behavior of S28 in Aqueous Solution. Materials. Pyrene (99% pure) was obtained from Aldrich, and poly(ethylene oxide) 35 000 was obtained from Fluka.

Methods. Static Light Scattering (SLS). SLS was performed on a Brookhaven BI-200 SM goniometer with a Lexel 95 Ar ion laser operating at 514 nm. Measurements were made at angles between 20 and 150°. The apparent weight-average molecular weight M_{app} was determined at each concentration from

$$1/M_{app} = Kc(I \times \sin \theta)_{\theta \rightarrow 0} \quad (1)$$

with

$$K = (dn/dc)^2 (4\pi^2 n_{tol}^2) I_{tol} / \lambda_0^4 N_a R_{tol} \quad (2)$$

I is the excess of scattering intensity of the solution as compared to the solvent, c is the concentration in polymer, in g/mL, λ_0 is the incident wavelength in vacuum, n_0 is the refractive index of the solvent, θ is the scattering angle, n_{tol} is the refractive index of toluene, I_{tol} is the intensity scattered by toluene at 90°, R_{tol} is the Rayleigh ratio for toluene, N_a is Avogadro's number, and dn/dc is the refractive index increment of the solution.

The solutions were prepared in Milli-Q water filtered through a 0.02 μm Anaport (Whatman) filter. The polymer solutions were stirred overnight and filtered through a 0.1 μm Anaport (Whatman) filter directly into the measurement cell.

The refractive index increment was determined for S28 in water with a KMX-16 differential refractometer (Chromatix) from measurements over the concentration range 10⁻³–10⁻² g/mL. A dn/dc value of 0.134 was found, which is very close to the value for PEG.

Dynamic Light Scattering (DLS). The polarized DLS measurements in the homodyne mode were performed using a 3 W Lexel 95 Ar ion laser operating at 514 nm. The intensity autocorrelation function $g_2(t)$ was measured at 90°, unless otherwise specified, using a BI-200SM goniometer version 2.0 and a 522 channel digital correlator BI-9000AT from Brookhaven. The correlator was used in the nonlinear mode. The minimum delay time accessible is 25 ns and the maximum 1.6 s. The temperature was set at 25 °C. The solutions were prepared in Milli-Q water and filtered through a 0.1 μm Anaport filter directly into the scattering cells.

The measured intensity autocorrelation function $g_2(t)$ is related to the electric field autocorrelation function $g_1(t)$ through the Siegert relation

$$g_2(t) = 1 + b g_1(t)^2 \quad (3)$$

where b is an instrumental parameter.

In all our experiments, we found that $g_1(t)$ could be described by a sum of two exponentials

$$b^{1/2} g_1(t) = a_f \exp(-\Gamma_f t) + a_s \exp(-\Gamma_s t) \quad (4)$$

where t is the delay time and (a_f , Γ_f) and (a_s , Γ_s) are the intensities and relaxation rates of the fast mode and the slow mode, respectively. The data were also analyzed using the Brookhaven CONTIN version 5.0 software which gives the

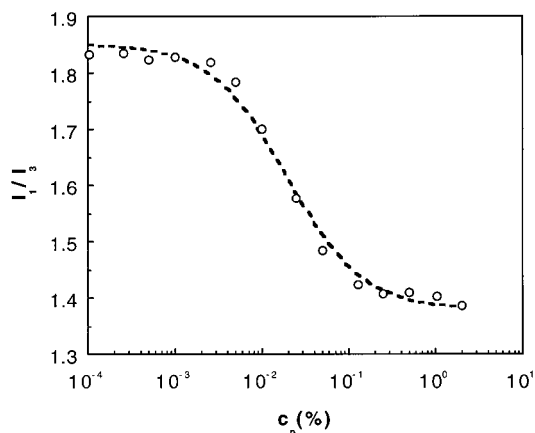


Figure 1. Variation of I_1/I_3 with c_p for S28. The curve represents the best fit of eq 6 to the data.

distribution of hydrodynamic diameters calculated from the diffusion coefficients using the Einstein relation for hard spheres.

Viscosity. The steady shear viscosities were measured at 25 °C using two different devices: a capillary viscometer (Ubbelohde, capillary diameter: 0.57 mm); a low shear rotational viscometer (Contraves LS30 used at shear rates from 0.5 to 100 s^{-1} with a Couette geometry).

The reduced viscosity, η_{red} , of the polymer was calculated from the formula

$$\eta_{red} = (\eta - \eta_0)/\eta_0 c \quad (5)$$

where η_0 is the viscosity of the solvent, η the viscosity of the solution, and c the concentration in polymer, expressed in g/mL.

Spectrofluorimetry.¹⁵ The fluorescence emission spectra of pyrene solubilized in the solutions were recorded in the range 350–500 nm at an excitation wavelength of 335 nm using a Shimadzu RF 5000 U spectrofluorimeter. The concentration of pyrene was 5×10^{-7} M. The ratio I_1/I_3 of the fluorescence intensity of the first and third emission peaks gives a measure of the polarity of the pyrene environment.¹⁶ I_1/I_3 was determined as a function of polymer concentration, to follow the association process.

Results and Discussion

Spectrofluorimetry. Figure 1 shows the plot of I_1/I_3 against polymer concentration. The I_1/I_3 transition occurs over a broad concentration range from about 5×10^{-6} M (0.004%) to 2.6×10^{-4} M (0.2%) where I_1/I_3 reaches a plateau value of 1.40. As also observed by others for hydrophobically end-capped PEO micelles,¹⁷ the plateau value is higher than for classical nonionic surfactants, suggesting relatively small hydrophobic domains. The decrease of I_1/I_3 stretches over nearly 2 orders of magnitude in concentration, in contrast to the decrease over a narrow range of concentration upon micellization for classical surfactants. Broad decreases of I_1/I_3 ratios have also been observed for hydrophobically end-capped PEO.^{17–19} An issue is whether the decrease locates the onset of association called the critical aggregation concentration (cac) or is due to a partition of the pyrene between water and the hydrophobic domains. If pyrene is partitioned between microdomains and water with a binding constant K and if the cac of the system is zero, then I_1/I_3 can be written as²⁰

$$I_1/I_3 = (I_1/I_3)_M + [(I_1/I_3)_w - (I_1/I_3)_M][1/(1 + Kc_p)] \quad (6)$$

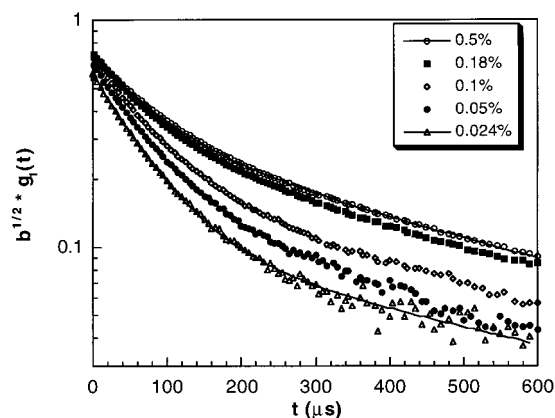


Figure 2. Time correlation functions $g_1(t)$ vs delay time measured at $\theta = 90^\circ$. From bottom to top: $c_p = 0.024, 0.05, 0.1, 0.18$, and 0.5% . The curves represent the fit of eq 4 to the data for $c_p = 0.024$ and 0.5% .

where $(I_1/I_3)_M$ and $(I_1/I_3)_w$ are the values in water and in the microdomains, respectively. (Equation 6 assumes additivity of fluorescence emission intensity, which, as pointed out by Acree,²¹ is true only if $I_{3,M} = I_{3,w}$. This assumption is reasonable for pyrene, since I_3 has been shown to vary very little with the pyrene environment.²²) The fit of the data with eq 6 is shown in Figure 1 with $K = 42\,700 \text{ mol}^{-1}$. The fairly good agreement between the calculated and experimental points supports the partitioning hypothesis, although the theoretical curve deviates slightly from the experimental results on both sides of the inflection point. Small deviations from the predictions of partitioning with a single binding constant have been observed in the case of amphiphilic block copolymer (the fluorescence quantity observed was not I_1/I_3 but the intensity ratio $I_{338}/I_{332.5}$ from the pyrene excitation spectra)²³ and interpreted as a manifestation of the micellization of the block copolymer. However, in solutions of polysoaps, which exhibit no cac (or more precisely a cac equal to zero), Anthony et al.²⁰ showed that such a variation could simply be ascribed to the dependence of K on the mole fraction of pyrene in the microdomains.

Static and Dynamic Light Scattering. The experiments were performed over a concentration range from 0.01 to 0.5%. Solutions were filtered through 0.1 μm filters, unless otherwise specified.

Dynamic Light Scattering. Figure 2 shows the correlation functions $g_1(t)$ at a scattering angle of $\theta = 90^\circ$ and for various concentrations. The functions are clearly not monoexponential. Over the entire concentration range, $g_1(t)$ can be fit by a sum of two exponentials, according to eq 4.

Examples of the fits are given in Figure 2 for the lowest (0.024%) and the highest (0.5%) polymer concentrations, c_p . For the highest concentration, $g_1(t)$ was measured at different angles. Both Γ_f and Γ_s were found to be proportional to the square of the scattering vector, q , showing diffusive processes, according to

$$D = \Gamma/q^2 \quad (7)$$

where D is a diffusion coefficient.

Table 2 gives the values of Γ_f , Γ_s , a_f (determined from the two exponential fits) as well as the hydrodynamic diameters d_{Hf} and d_{Hs} determined according to

$$d_H = kT/3\pi\eta D \quad (8)$$

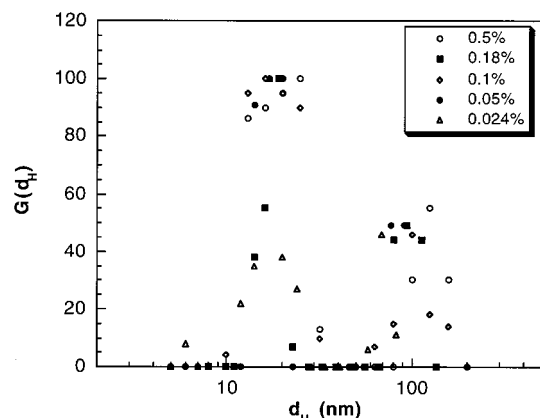


Figure 3. CONTIN distribution of the hydrodynamic diameters. $c_p = 0.024\%$ (Δ), 0.05% (\bullet), 0.1% (\diamond), 0.18% (\blacksquare), and 0.5% (\circ).

Table 2. Relaxation Rate, Relative Intensity, and Hydrodynamic Diameters Corresponding to the Fast and Slow Mode as a Function of Polymer Concentration

c_p (%)	Γ_f (μs^{-1})	d_{Hf} (nm)	Γ_s (μs^{-1})	d_{Hs} (nm)	a_f (% tot. intens)
0.024	0.0154	16.9	0.00205	126.8	79.8
0.05	0.0149	17.4	0.00236	109.7	74
0.1	0.0140	18.6	0.00209	123.9	71.8
0.18	0.0140	18.6	0.00216	120.1	58.8
0.5	0.0129	20.0	0.00205	126.7	57.0

where k is the Boltzmann constant, T the temperature, and η the viscosity of the solution. d_{Hf} varies very little with concentration, increasing from 16.9 nm at $c_p = 0.024\%$ to 20 nm at $c_p = 0.5\%$. Values of d_{Hs} fluctuate between 110 and 127 nm, which, within experimental error, corresponds to the filter pore size (100 nm) and suggests that aggregates of larger sizes may have been retained by the filter. However, no measurable mass loss after filtration was observed. The relative intensity related to the fast mode decreases when c_p increases, from 80% at $c_p = 0.024\%$ to 57% at $c_p = 0.5\%$.

The distribution of the hydrodynamic diameters $G(d_H)$ obtained using CONTIN is given in Figure 3. The distributions are clearly bimodal, at all concentrations. The maximum of the first peak is around 16 to 20 nm and the maximum of the second peak around 100 nm, in good agreement with the results of the "two-exponential" fit.

We first discuss the origin of the fast mode in the relaxation spectra. Devanand and Selser report for PEO in water at 30°C ²⁴

$$R_H = 0.145M_w^{0.571} (\text{\AA}) \quad (9)$$

which gives a hydrodynamic diameter $d_H = 10.4$ nm for unmodified PEO of molecular weight 28 000. This is approximately half the value of d_{Hf} given by the "two-exponential" fits or the maximum of the first peak (i.e., fast mode) of the distribution given by CONTIN. Thus, the fast mode appears to arise from associated polymer. We will show later that the size measured is compatible with the size of one flowerlike micelle. As d_{Hf} does not vary with c_p , the micelle size is independent of concentration. The distribution given by CONTIN in Figure 3 shows that $G(d_H)$ is almost equal to zero for $d_H < 10$ nm, for all the concentrations studied. Since a nonassociating PEO chain of $M_w = 28$ 000 would have a d_H of 10 nm and a single chain with intramolecular associations would have a smaller size than 10 nm, this

means that almost all the polymer is present in the form of aggregates even at the smallest concentration studied. It can be shown that most of the polymer is associated with the micelles responsible for the fast mode; in first approximation

$$c_s/c_f = (a_s/a_f)(M_f/M_s) \quad (10)$$

where (c_f, M_f) and (c_s, M_s) are the weight concentrations and the weight-average molecular weights of the species associated with the fast and slow modes, respectively. By assuming constant density, we can estimate the relative weight concentrations of polymer associated with the two modes

$$c_s/c_f = (a_s/a_f)(d_{Hf}/d_{Hs})^3 \quad (11)$$

and thus c_s represents a maximum of 0.3% of c_f (calculated for $c_p = 0.5\%$, where a_s/a_f has its highest value).

For the slow mode, the hydrodynamic diameter extracted from Γ_s is approximately 120 nm, at all c_p , and indicates that the slow mode is due to large aggregates which are comparable in size to the pore size of the filter. Another series of measurements was made on solutions filtered through $0.45 \mu\text{m}$ filters. As compared to the solutions filtered through $0.1 \mu\text{m}$ filter, the decay of the autocorrelation function was much slower, showing the presence of larger aggregates. The CONTIN analysis still showed two peaks. The peak corresponding to the fast mode was unchanged, whereas the one for the slow mode was extended to higher diameters, and the relative intensity of the slow mode was considerably enhanced. Filtration through $0.1 \mu\text{m}$ filter partially removed the large aggregates present in solution, whereas it did not affect the fast mode attributed to polymer contained within individual micelles.

The partial elimination of the slow mode by filtration through a small pore size filter suggests that the slow mode is not due to a thermodynamic equilibrium. Since no measurable mass loss was detected after filtration, isolation and characterization of the sample fraction responsible for the slow mode were not possible. The phase behavior of S113, which has a structure similar to that of S28, but a higher molecular weight, is described in another publication.²⁵ Phase separation between a gellike phase and a dilute solution occurs. The weight-average molecular weight of the polymer fraction contained in the solution phase was shown to be lower than that of the polymer contained in the gel phase. This suggests a possible explanation for the origin of the slow mode in solutions of S28: The small number of high molecular weight chains present in the solution may be involved in the formation of highly connected micelles, which would form a microgel fraction. By filtration, that fraction is irreversibly removed from the solution. However, alternate explanations are possible. A slow mode has been observed in solutions of nonmodified PEO,²⁶⁻²⁸ and its origin has been the subject of controversy. Attributed first to aggregation of PEO even in dilute water solution, it has been shown more recently^{26,28} that it could be attributed to the presence of an impurity and could be removed by filtration through a sufficiently small filter size. Alami et al. observed a slow mode in dilute solutions of hydrophobically end-capped PEO¹⁷ and noticed that it could be almost completely removed by addition of a small amount of NaCl. They concluded, therefore, that

Table 3. Apparent Molecular Weight, M_{app} , Average Aggregation Number, and Corrected Aggregation Number at Different Polymer Concentrations

c_p (%)	$M_{app} \times 10^{-5}$	$N_R(av)$	$N_R(corr)$
0.024	1.25	14.9	11.9
0.05	1.50	17.9	13.2
0.10	1.65	19.6	14.1
0.18	2.06	24.6	14.5
0.50	2.11	25.1	14.3

it may be inherent to the presence of PEO itself, rather than to the hydrophobic moieties.

Static Light Scattering. The variation of M_{app} with polymer concentration is given in Table 3. M_{app} is higher than the weight-average molecular weight determined by GPC in DMF in which the chain and hydrophobe are nonassociating and completely dissolved. M_{app} increases with the concentration, going from 1.25×10^5 for $c_p = 0.024\%$ to 2.11×10^5 for $c_p = 0.5\%$. Even at the lowest concentration studied, the molecular weight of the aggregates is already 4 times higher than the molecular weight of the single chain. It is difficult to distinguish whether the increase of M_{app} with c_p reflects an increase of the molecular weight with c_p or a negative second virial coefficient. If we assume that the effect is due to aggregation, the average aggregation number in terms of the number of hydrophobes per aggregate, N_R , increases from 15 at the lowest concentration to 25 at the highest concentration studied. As a first approximation, the scattered intensity can be written as

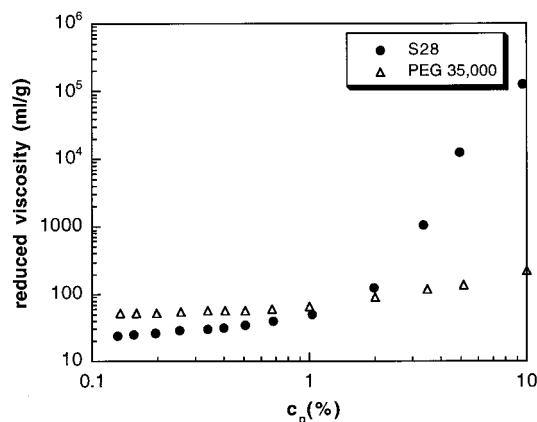
$$I = I_{mic} + I_{agg} \quad (12)$$

where I_{mic} and I_{agg} are the intensities scattered by the micelles and the large aggregates, respectively, and

$$A_f = I_{mic}/I \quad A_s = I_{agg}/I \quad (13)$$

where A_f and A_s are the relative intensities of the fast and slow mode determined by dynamic light scattering. M_{app} (micelle) is determined by replacing I by $I_{mic} = IA_f$ in eq 1.

After subtraction of the intensity associated with the larger aggregates, the corrected values of N_R are between 12 and 14 and are nearly independent of c_p . For the calculation of N_R , we used the molecular weight of the PEG₈₀₀₀–lysine–stearylamine repeat unit. The slight excess of PEG revealed by NMR was not taken into account, because the excess may have two possible origins which would affect the N_R value in an opposite way. In the extreme case where the excess is entirely due to the fact that chains are terminated more by PEG than by lysine–stearylamine, N_R is overestimated by approximately 20%, whereas it is underestimated by approximately 20% if the excess is entirely due to a small amount of unreacted PEG 8000. For micelles of hydrophobically end-capped PEO, a rather broad range of values (most often determined by fluorescence techniques) are reported in the literature: Yekta et al.²⁹ found $N_R = 20 \pm 2$ for HEUR polymers with M_n ranging from 34 000 to 50 000 with $C_{16}H_{33}$ end groups. Alami et al. reported values between 15 and 30 for C_{12} –EO₄₆₀– C_{12} , and Person et al. measured values of 31 ± 6 by electron paramagnetic resonance spectroscopy for C_{12} –EO₂₀₀– C_{12} .³⁰ The random comblike copolymer comb-81 described by Xu et al., with $C_{14}H_{29}$ pendant groups separated by PEG spacers of $M = 8400$, forms flowerlike micelles of aggregation number 15, very close to the

**Figure 4.** Reduced viscosity vs polymer concentration: S28 (●); PEG 35 000 (Δ).

value that we found for S28 in the same concentration range.

The size of one flowerlike micelle with a hydrophobic core containing 14 hydrocarbon tails with 18 carbons surrounded by a corona of PEG chain loops swollen by the solvent can be estimated as follows:

The volume V_c of the hydrophobic core is obtained using the Tanford equation,³¹ which gives the volume of a hydrocarbon chain with n carbon atoms:

$$v = (27.4 + 26.9n) \times 10^{-3} \text{ nm}^3 \quad (14)$$

Hence, $V_c = N_R v = 7.16 \text{ nm}^3$, with $N_R = 14$ and $n = 18$.

This gives the radius of the core, $R_c = 1.19 \text{ nm}$. The thickness of the corona, R_{cor} , is given by the dimension of the PEG spacer. Since the hydrophobic groups are closely packed, the loops crowd each other. This crowding results in a stretching of the loops in the outward direction. It is predicted^{32,33} that the thickness of the corona is increased by a factor of $N_R^{1/5}$ compared to the dimension of the unperturbed spacer chain, which can be estimated from eq 9. This relation gives a hydrodynamic diameter of 4.9 nm for PEG 8000, which leads to $R_{cor} = 8.3 \text{ nm}$ with $N_R = 14$. The hydrodynamic diameter of the flowerlike micelle is $2(R_c + R_{cor}) = 19 \text{ nm}$, in good agreement with d_H measured by DLS.

Viscosity. Measurements were performed using the capillary viscometer after filtration of the solutions through $0.2 \mu\text{m}$ filters for $c_p < 1\%$, and using the low shear viscometer on unfiltered solutions at higher polymer concentrations.

The reduced viscosity in water is given as a function of concentration in Figure 4. As a comparison, the results for PEG homopolymer of molecular weight 35 000 is given on the same plot. The intrinsic viscosity, $[\eta]$, has been calculated in the low concentration range according to the following relation:

$$(\eta - \eta_0)/\eta_0 c = [\eta](1 + k[\eta]c + \dots) \quad (15)$$

For the comb polymer, $[\eta] = 21.0 \text{ mL/g}$ and $k = 6.15$, whereas for the PEG homopolymer $[\eta] = 50.6$ and $k = 0.56$. The value of k for the comb polymer is much greater than the values expected for a flexible linear polymer (between 0.3 and 0.8). The low values of the reduced viscosity at c_p less than 1% compared to PEG homopolymer, coupled with light-scattering data which shows that the weight-average molecular weight of the aggregates is much higher than 35 000, indicate a compact associated aggregate.

The light-scattering study shows that the main species in solution is a micelle composed nominally of four to five polymer chains. The large aggregates responsible for the slow mode are present in very small amounts and should not play a significant part in the intrinsic viscosity. Knowing the hydrodynamic diameter of the micelles ($d_H = 18$ nm), the Einstein relation for hard spheres

$$[\eta] = 2.5 VM \quad (16)$$

where V and M are the volume and molecular weight of one micelle, respectively, leads to $M = 175\,000$, corresponding to a N_R of about 21, slightly higher than the value of 14 deduced from the light-scattering study.

At concentrations higher than 1%, the viscosity of the comb polymer increases rapidly and becomes higher than the viscosity of PEG homopolymer. For both polymers, the viscosity increases more rapidly with c_p for concentrations higher than 1–2%. This range of concentration coincides with the overlapping concentration c^* of the chains (given by the reciprocal of the intrinsic viscosity) of the homopolymer, but is well below the c^* (=5%) of the primary flowerlike micelles of the comb polymer.

Conclusion

We have synthesized a family of new strictly alternating, amphiphilic comb copolymers. The design of these copolymers allows the independent variation of molecular weight while maintaining constant hydrophilic block length and a constant ratio of hydrophilic blocks to hydrophobe graft sites. We have investigated the association in water of a copolymer with pendent $C_{18}H_{37}$ hydrophobic groups separated by PEG of molecular weight 8000, in which each chain contains on average two to three hydrophobic groups. At low concentrations S28 associates mainly in the form of individual flowerlike micelles containing an average of four to five chains and a total of approximately 14 hydrophobic units. Onset of association was too low to be detected, but is below than 0.025%, the lowest concentration studied by light scattering. At concentration higher than 2%, the system exhibits large increase in viscosity, indicating the formation of larger aggregates.

Acknowledgment. This work was supported by a seed grant from the New Jersey Center for Biomaterials and Medical Devices, by the New Jersey Commission on Science and Technology, and by NIH Grant GM39455. Mr. D. Kruckner synthesized the low molecular weight sample (S28). The authors thank the scientific staff of the Complex Fluids Laboratory at Rhodia, Inc., for stimulating discussions and for access to the light-scattering apparatus and the low shear viscosimeter. The authors also thank Mr. D. E. Weyand for access to the static fluorimeter and Professor M. Hara for access to the refractometer.

References and Notes

- (1) Kramer, M.; Stefer, J.; Hu, Y.; McCormick, C. *Macromolecules* **1996**, *29*, 1992.
- (2) Magny, B.; Illiopoulos, I.; Audebert, R. In *Macromolecular Complexes in Chemistry and Biology*; Dubin, P., Bock, J., Davis, R., Schultz, D., Thies, C., Eds.; Springer-Verlag: Berlin, 1994; pp 51–62.
- (3) Selb, J.; Biggs, S.; Renoux, D.; Candau, F. In *Hydrophilic Polymers*; Glass, J. E., Ed.; American Chemical Society: Washington, DC, 1996; pp 251–278.
- (4) Landoll, L. M. *J. Polym. Sci., Polym. Chem. Ed.* **1982**, *20*, 443.
- (5) Thuresson, K.; Nilsson, S.; Lindman, B. *Langmuir* **1996**, *12*, 2412.
- (6) Xu, B.; Li, L.; Zhang, K.; Macdonald, P. M.; Winnik, M. A. *Langmuir* **1997**, *13*, 6896–6902.
- (7) Xu, B.; Yekta, A.; Winnik, M. A.; Sadeghy-Dalivand, K.; James, D. F.; Jenkins, R.; Bassett, D. *Langmuir* **1997**, *13*, 6903–6911.
- (8) Glass, J. E.; Fernando, R. H.; Eglund-jongewaard, S. K.; Brown, R. G. *J. Oil Colour Chemist. Assoc.* **1984**, *67*, 256–561.
- (9) Jenkins, R. D. Ph.D. Thesis, Lehigh University, Bethlehem, PA, 1991.
- (10) Annable, T.; Buscall, R.; Ettelaie, R.; Whittlestone, D. *J. Rheol.* **1993**, *37*, 695–726.
- (11) Kaczmariski, J. P.; Glass, J. E. *Macromolecules* **1993**, *26*, 5149–5156.
- (12) Alami, E.; Rawiso, M.; Isel, F.; Beinert, G.; Binana-Limbele, W.; Francois, J. In *Hydrophilic Polymers*; Glass, J. E., Ed.; American Chemical Society: Washington, DC, 1996; pp 343–362.
- (13) Nathan, A.; Bolikal, D.; Vyavahare, N.; Zalipski, S.; Kohn, J. *Macromolecules* **1992**, *25*, 4476–4484.
- (14) Zalipsky, S.; Seltzer, R.; Menon-Rudolph, S. *Biotechnol. Appl. Biochem.* **1992**, *15*, 100.
- (15) Zana, R. In *Surfactant Solutions*; Zana, R., Ed.; Marcel Dekker: New York and Basel, Switzerland, 1987; pp 241–294.
- (16) Kalyanasundaram, K.; Thomas, J. K. *J. Am. Chem. Soc.* **1977**, *99*, 2039.
- (17) Alami, E.; Almgren, M.; Brown, W.; Francois, J. *Macromolecules* **1996**, *29*, 2229–2243.
- (18) Maitre, S. Ph.D. Thesis, Université Louis Pasteur, Strasbourg, France, 1997.
- (19) Wang, Y.; Winnik, M. A. *Langmuir* **1990**, *6*, 1437–1439.
- (20) Anthony, O.; Zana, R. *Macromolecules* **1994**, *27*, 3885–3891.
- (21) Acree, W. E.; Tucker, S. A.; Wilkins, D. C. *Macromolecules* **1993**, *26*, 7366.
- (22) Kalyanasundaram, K.; Thomas, J. K. *J. Am. Chem. Soc.* **1977**, *99*, 2039.
- (23) Wilhelm, M.; Zhao, C.-L.; Wang, Y.; Xu, R.; Winnik, M. A.; Mura, J.-L.; Riess, G.; Croucher, M. D. *Macromolecules* **1991**, *24*, 1033–1040.
- (24) Devanand, K.; Selser, J. C. *Macromolecules* **1991**, *24*, 5943.
- (25) Heitz, C.; Prudhomme, R. K.; Kohn, J. *Macromolecules* **1999**, *32*, 6658.
- (26) Devanand, K.; Selser, J. C. *Nature* **1990**, *343*, 739.
- (27) Polik, W. F.; Burchard, W. *Macromolecules* **1983**, *16*, 976.
- (28) Porsch, B.; Sundelof, L. O. *Macromolecules* **1995**, *28*, 7165–7170.
- (29) Yekta, A.; Xu, B.; Duhamel, J.; Adiwidjaja, H.; Winnik, M. *Macromolecules* **1995**, *28*, 956–966.
- (30) Persson, K.; Bales, B. L. *J. Chem. Soc., Faraday Trans.* **1995**, *91*, 2863–2870.
- (31) Tanford, C. *The Hydrophobic Effect*; Wiley: New York, 1973.
- (32) Daoud, M.; Cotton, J. P. *J. Phys. Fr.* **1982**, *43*, 531.
- (33) Borisov, O. V.; Halperin, A. *Langmuir* **1995**, *11*, 2911–2919.

MA991158A